DJ-1 deficiency impairs synaptic vesicle endocytosis and reavailability at nerve terminals

Jae Won Kyung[a,1], Jin-Mo Kim[b,c,1], Wongyoung Lee[d], Tae-Young Ha[b,c], Seon-Heui Cha[b,c], Kyung-Hwun Chung[e], Dong-Joo Choi[b,c,f], Ilo Jou[b,c,f], Woo Keun Song[e], Eun-Hye Joe[b,c,f], Sung Hyun Kim[g,2], and Sang Myun Park[b,c,f,2]

[a]Department of Biomedical Science, Graduate School, Kyung Hee University, 02447 Seoul, Korea; [b]Department of Pharmacology, Ajou University School of Medicine, 16499 Suwon, Korea; [c]Chronic Inflammatory Disease Research Center, Ajou University School of Medicine, 16499 Suwon, Korea; [d]Department of Neuroscience, Graduate School, Kyung Hee University, 02447 Seoul, Korea; [e]School of Life Science, Bio Imaging and Cell Dynamics Research Center, Gwangju Institute of Science and Technology, 61005 Gwangju, Korea; [f]BK21 Plus Program, Department of Biomedical Sciences, Ajou University School of Medicine, 16499 Suwon, Korea; and [g]Department of Physiology, School of Medicine, Kyung Hee University, 02447 Seoul, Korea

Edited by Solomon H. Snyder, The Johns Hopkins University School of Medicine, Baltimore, MD, and approved January 5, 2018 (received for review May 26, 2017)

Mutations in DJ-1 (PARK7) are a known cause of early-onset autosomal recessive Parkinson's disease (PD). Accumulating evidence indicates that abnormalities of synaptic vesicle trafficking underlie the pathophysiological mechanism of PD. In the present study, we explored whether DJ-1 is involved in CNS synaptic function. DJ-1 deficiency impaired synaptic vesicle endocytosis and reavailability without inducing structural alterations in synapses. Familial mutants of DJ-1 (M26I, E64D, and L166P) were unable to rescue defective endocytosis of synaptic vesicles, whereas WT DJ-1 expression completely restored endocytic function in DJ-1 KO neurons. The defective synaptic endocytosis shown in DJ-1 KO neurons may be attributable to alterations in membrane cholesterol level. Thus, DJ-1 appears essential for synaptic vesicle endocytosis and reavailability, and impairment of this function by familial mutants of DJ-1 may be related to the pathogenesis of PD.

DJ-1 | Parkinson's disease | synaptic vesicle endocytosis | synaptic vesicle reavailability

Parkinson's disease (PD) is recognized as the second most-common neurodegenerative disease after Alzheimer's disease, and characterized by progressive degeneration of dopaminergic neurons in the substantia nigra pars compacta, leading to dopamine depletion in the striatum and the presence of intracytoplasmic inclusions known as Lewy bodies and Lewy neurites (1). Although the pathogenesis of PD remains to be fully elucidated, monogenic forms of PD caused by mutations in several genes, including *SNCA*, *parkin*, *PINK1*, *LRRK2*, and *DJ-1*, have been identified. Moreover, the list of PD-associated genes continues to grow, providing valuable insights into the pathogenesis of the disease (1).

Modulation and alteration of synaptic physiology are tightly related in PD. Impaired efficacy of synaptic transmission in striatum plays a role in the acquisition of PD phenotype, and altered synaptic vesicle (SV) trafficking is evident in some PD models (2). Associations of gene products found in familial PD—such as α-synuclein (3–5), parkin (6, 7), and LRRK2 (8, 9)—with SV trafficking have been reported. In addition, monogenic mutations of *synj1* (PARK20) (10, 11) and *DNAJC6* (PARK19) (12, 13) encoding the endocytic proteins, synaptojanin-1 and auxilin, respectively, were recently identified in patients with atypical parkinsonism. Recent genome-wide association studies have suggested that dysfunction in synaptic transmission and sorting are convergent processes in late-onset PD (14), supporting the theory that abnormal SV trafficking is potentially a common pathophysiological mechanism of PD.

DJ-1, also known as PARK7, is a multifunctional protein. Mutations in DJ-1, such as M26I, E64D, and L166P, have been identified in the rare early-onset autosomal recessive type of familial PD (15). DJ-1 is ubiquitously expressed in various tissues, including brain, and implicated in several processes, including cell cycle regulation and oncogenesis, control of gene transcription, and response to cell stress, in a cell type-specific manner (15). In neurodegeneration, DJ-1 functions as an antioxidant or sensor of oxidative stress (15). While DJ-1 is mainly localized in the cytosol, its presence in axons, dendrites, and presynaptic terminals has also been documented (16). Moreover, the protein associates with the synaptic membrane (17), suggesting a role in synaptic transmission, which remains to be explored.

In the present study, we examined whether DJ-1 is involved in synaptic function and shares a common pathological mechanism with other PD-associated gene products. In the absence of DJ-1, SV endocytosis was significantly altered and SV reavailability was impaired. Moreover, DJ-1 KO neurons expressing pathogenic mutants of DJ-1 were unable to repair the impaired kinetics of SV endocytosis, whereas WT DJ-1 expression completely restored this endocytic defect. Our findings clearly support a critical role of DJ-1 in SV trafficking.

Results

DJ-1 Localizes at Presynaptic Terminals in Primary Cultured Neurons. Although DJ-1 is reported to be present within striatal axons, presynaptic terminals, and dendritic spines (16), and where it associates with synaptic membranes (17), detailed colocalization

Significance

Synaptic dysfunction is implicated as a major causative factor in neurodegenerative diseases. We focused on the role of DJ-1, a genetic factor for early-onset autosomal recessive Parkinson's disease, in synaptic vesicle endocytosis. DJ-1 was localized at nerve terminals. In the absence of DJ-1, synaptic vesicle endocytosis and reavailability were severely impaired with no alteration of the structural characteristics of nerve terminals, implying an important role in synaptic vesicle recycling. Intriguingly reexpression of several familial mutants (M26I, E64D, and L166P) of DJ-1 identified in Parkinson's disease failed to restore synaptic vesicle recycling in DJ-1 KO neurons. Our data collectively indicate that DJ-1 participates in synaptic vesicle endocytosis, and pathogenic mutants of DJ-1 are potentially linked to the synaptic retrieval pathway.

Author contributions: J.W.K., J.-M.K., W.L., S.H.K., and S.M.P. designed research; J.W.K., J.-M.K., W.L., T.-Y.H., S.-H.C., K.-H.C., D.-J.C., and S.H.K. performed research; I.J., W.K.S., E.-H.J., and S.H.K. contributed new reagents/analytic tools; J.W.K., T.-Y.H., D.-J.C., I.J., W.K.S., E.-H.J., S.H.K., and S.M.P. analyzed data; and S.H.K. and S.M.P. wrote the paper.

The authors declare no conflict of interest.

This article is a PNAS Direct Submission.

[1]J.W.K. and J.-M.K. contributed equally to this work.

[2]To whom correspondence may be addressed. Email: sunghyunkim@khu.ac.kr or sangmyun@ajou.ac.kr.

This article contains supporting information online at www.pnas.org/lookup/suppl/doi:10.1073/pnas.1708754115/-/DCSupplemental.

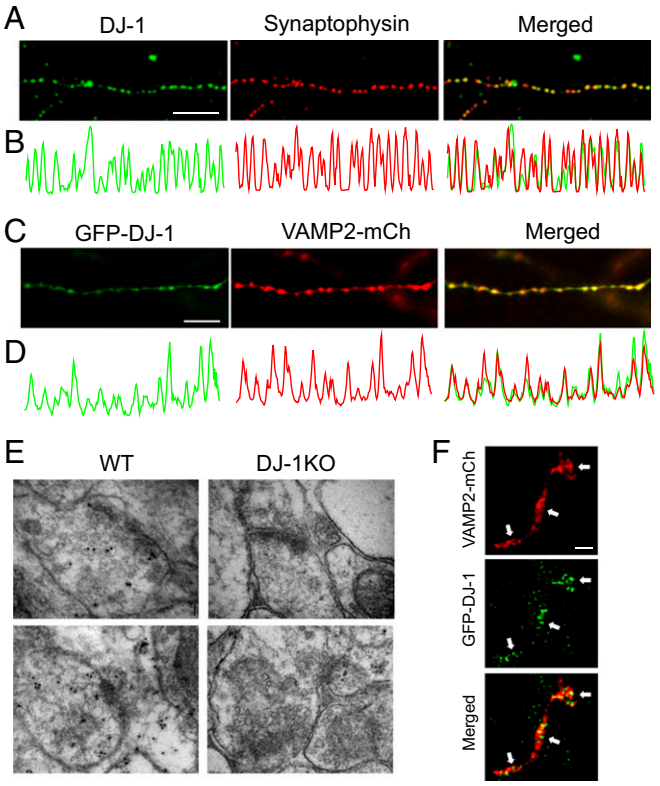

Fig. 1. DJ-1 localizes at the nerve terminals of primary cultured neurons. (*A*) Representative images of DJ-1 and synaptophysin immunocytochemistry. Mouse cortical neurons were fixed and double-stained with anti–DJ-1 (green) and antisynaptophysin (red) antibodies, followed by Alexa-labeled secondary antibodies (Alexa-488 and Alexa-546). (*C*) Representative images of GFP–DJ-1 with VAMP2-mCherry, a nerve terminal marker, transfected and expressed in mouse cortical neurons. (Scale bars, 5 μm.) (*B* and *D*) Line-scan profiles of DJ-1 and synaptophysin (*B*) or GFP–DJ-1 and VAMP2-mCherry (*D*). (*E*) Representative immunogold EM images of DJ-1 in WT and DJ-1 KO brain slices. (Scale bar, 50 nm.) (*F*) Representative superresolution images of GFP–DJ-1 and VAMP2-mCherry obtained using HyVolution. Arrows indicate localization of GFP–DJ-1 with the presynaptic marker VAMP2-mCh at nerve terminals. (Scale bar, 1 μm.)

studies have not been carried out to date. We verified the presence of DJ-1 in presynaptic terminals of primary cultured neurons. Initially, we examined whether DJ-1 is located at presynaptic terminals, a hot-spot of SV trafficking for functional neural communication. DJ-1 strongly colocalized with synaptophysin, a SV-associated membrane protein, at synaptic boutons (Fig. 1 *A* and *B*). Exogenously expressed GFP–DJ-1 and VAMP2-mCherry in primary cultured cortical neurons also showed highly overlapping signals (Fig. 1 *C* and *D*). The distribution of DJ-1 was significantly correlated with the size of synaptic boutons (Fig. S1), and DJ-1 was relatively enriched in synapses compared with axons (Fig. S2). In addition, immunogold labeling for DJ-1 by electron microscopy (EM) was carried out in WT and DJ-1 KO mouse brains. DJ-1^{+} immunogold particles were detected in WT brains, where they were localized at synapses; in contrast, EM images showed no such gold particles in the DJ-1 KO brain (Fig. 1*E*). Superresolution imaging also revealed that GFP–DJ-1 localization partially overlapped with or was adjacent to (i.e., within several hundred nanometers) that of VAMP2-mCherry (Fig. 1*F* and Fig. S2), suggesting that DJ-1 localizes to nerve terminals and may participate in synaptic functions, such as SV trafficking.

The Ultrastructure of Nerve Terminals Does Not Differ Between WT and DJ-1 KO Neurons. To establish whether DJ-1 deficiency alters the structural state of presynaptic terminals, EM was employed to determine synapse ultrastructure. The number of SV in the vicinity of the active zone (AZ; ~100 nm) was not significantly different between WT and DJ-1 KO neurons (Fig. 2 *A*–*C*). The length of AZ was distinctively stained as a dark line in the plasma membrane, and SV diameters were approximately similar between WT and DJ-1 KO neurons (Fig. 2 *D* and *E*), implying that DJ-1 does not contribute to synaptic structure formation. We additionally measured the population of functional SV released during neural activities. Staining with FM1-43, an amphipathic

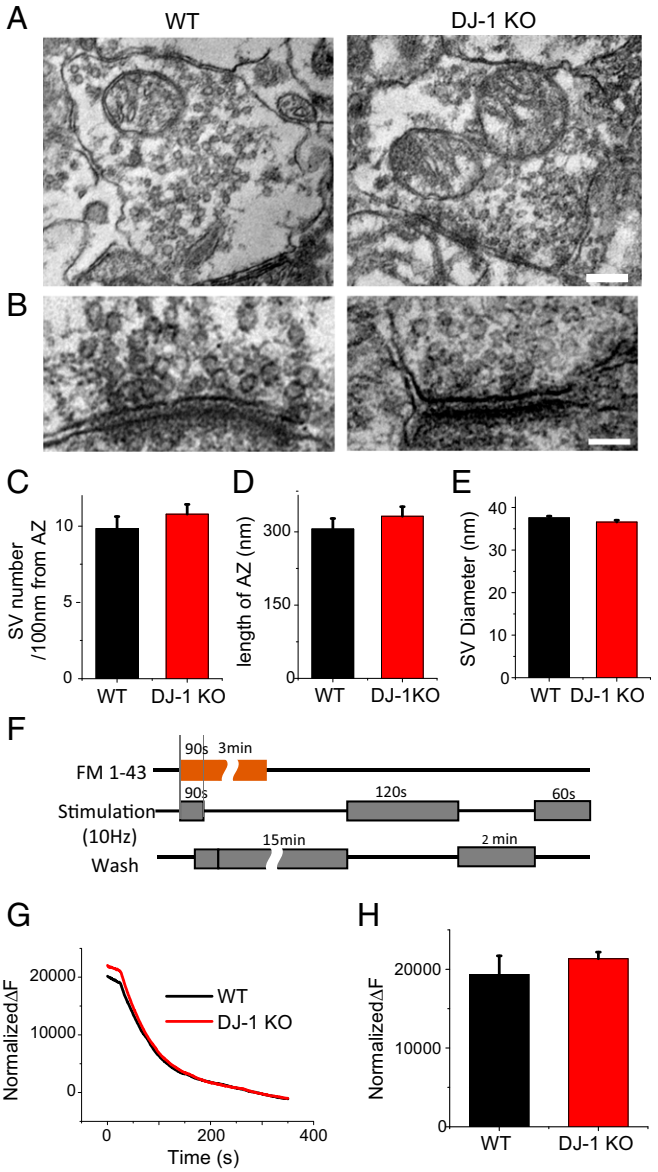

Fig. 2. Ultrastructures of synapses are not altered between WT and DJ-1 neurons. (*A*) Representative ultrastructure images of nerve terminals in the cortex from WT (*Left*) and DJ-1 KO brain (*Right*). (*B*) Enlarged images of AZ ultrastructures of WT (*Left*) and DJ-1 KO (*Right*). (Scale bars, 100 nm.) (*C*–*E*) Quantitative analysis of mean SV numbers in the vicinity of AZ (~100 nm) (*C*), length of AZ (*D*), and diameter of SV (*E*) from WT and DJ-1 KO synapses. (*F*) Schematic diagram of measurement of the total recycling pool of SVs using FM1-43. (*G*) Traces of FM1-43 unloading from WT and DJ-1 neurons. Neurons maximally loaded with FM1-43 via prolonged stimulation (900 AP at 10 Hz) to label total recycling of SVs were subjected to sequential stimulation (1,200 AP and 600 AP at 10 Hz) for unloading of FM1-43. (*H*) Mean maximal FM1-43 signal intensity.

membrane-selective dye, revealed that the total recycling pool sizes of SV were indistinguishable (Fig. 2 *F–H*). Furthermore, the entire population of SV was similar between groups (Fig. S3). Therefore, DJ-1 does not appear to participate in the structural organization of nerve terminals.

SV Endocytosis Is Significantly Defective in DJ-1 KO Neurons. Next, we examined the potential role of DJ-1 in SV trafficking using primary cultured cortical neurons from DJ-1 KO or WT mice transfected with vGlut1-pHluorin (vG-pH). Fluorescence of pHluorin, a mutant form of GFP, is quenched by protonation (~pK_a 7.1). Upon fusing this protein to the luminal region of SV membrane proteins (e.g., vGlut1), fluorescence of pHluorin can be unquenched by activity-driven SV exocytosis. Following exocytosis, SV endocytosis can be traced by signal decay due to recapture of the pHluorin-tagged SV protein and vesicle reacidification (18). To quantify the kinetics of poststimulus SV endocytosis, we monitored the time-course of vG-pH fluorescence decay following action potential firing. In WT presynaptic terminals, poststimulus vG-pH fluorescence decay was fit to a single exponential decay with a time constant of 13.40 ± 0.83 s. In DJ-1 KO presynaptic terminals, the signal decay of vG-pH was significantly slower with a time constant of 25.46 ± 0.37 s (Fig. 3 *A* and *B*). Consistently, analysis of individual synaptic boutons revealed defective kinetics of SV endocytosis in DJ-1 KO neurons (Fig. 3*C*). We additionally examined for defects in SV endocytosis during neural activity in DJ-1 KO neurons. The vG-pH response to 30-s stimulation at 10 Hz with or without bafilomycin (BAF) was compared in WT and DJ-1 KO neurons. Comparison of these two signals ($\Delta F_{BAF+} - \Delta F_{BAF-}$) enables calculation of the extent of endocytosis during a given stimulation (19). In DJ-1 KO neurons, the amount of endocytosis during the stimulation period was significantly decreased (~threefold lower) compared with WT neurons (Fig. 3 *D–F*).

To establish whether this endocytic defect is specifically attributable to DJ-1 depletion, DJ-1 KO neurons were cotransfected with vG-pH and cDNA encoding WT DJ-1. Analysis of vG-pH fluorescence decay kinetics following stimulation showed that the endocytic defect was completely rescued upon reexpression of WT DJ-1 (Fig. 3 *G–I*). Based on these findings, we concluded that DJ-1 plays an important role in SV endocytosis during and after neural activity.

We additionally investigated whether DJ-1 participates in SV exocytosis. Exocytosis assays were performed by examining the amplitude of vG-pH responses following brief [100 action potentials (AP)] or prolonged stimulation. Although vG-pH signals represent the balance of exocytosis and endocytosis, we previously demonstrated that the contribution of endocytosis is minimal during 10-s stimulation at 10 Hz (20). The amplitude of the vG-pH signal was normalized to the maximal possible fluorescence signal obtained by brief perfusion with NH_4Cl to alkalinize the entire recycling pool. For the longer stimulation protocol, we used BAF to block SV reacidification, which renders the vG-pH signal blind to any endocytosis event, thus solely revealing the kinetics of exocytosis of the entire recycling pool (20). These experiments showed that loss of DJ-1 does not impact SV exocytosis and the associated kinetics with either stimulus regime (Fig. S4), suggesting that the protein does not function in SV exocytosis.

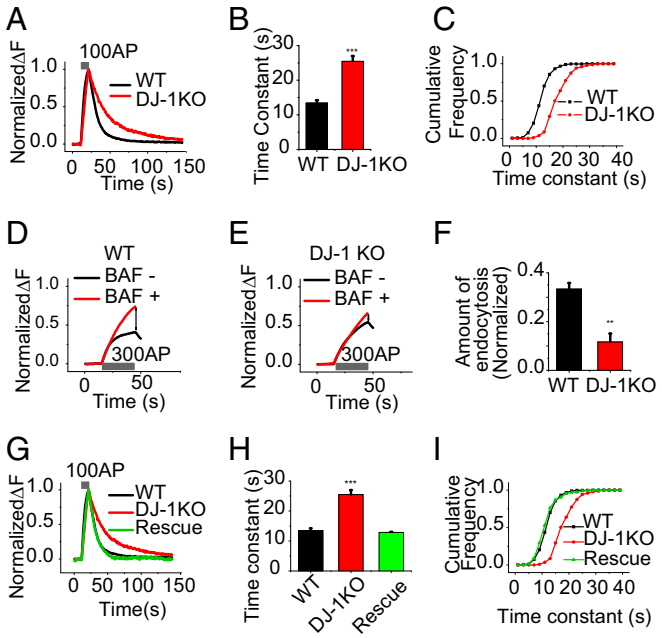

Fig. 3. SV endocytosis is altered in DJ-1 KO neurons. (*A*) Representative traces of endocytosis from WT and DJ-1 KO neurons. Neurons transfected with vG-pH were stimulated at 10 Hz for 10 s (100 AP). (*B*) Mean time constants of poststimulus endocytosis from WT (τ_{endo} = 13.40 s ± 0.83 s; n = 20 cells) and DJ-1 KO (τ_{endo} = 25.46 s ± 0.37 s; n = 30 cells) neurons. ***$P < 0.001$. (*C*) Cumulative frequency of time constants from a single bouton from WT (black) and DJ-1 KO neurons. (*D* and *E*) Representative trace of vG-pH response to 300 AP from WT (*D*) and DJ-1 KO (*E*) neurons in the presence (red) or absence (black) of BAF A1. (*F*) Mean values of the extent of endocytosis during 30 s of activity in WT and DJ-1 KO neurons (~threefold lower in DJ-1 KO neurons, compared with WT neurons). (*G*) Representative trace of vG-pH responses to 100 AP from WT (black), DJ-1 KO (red) and rescue (green) neurons. Cells transfected with vG-pH with/without DJ-1 cDNA were stimulated at 10 Hz for 10 s. (*H*) Mean time constants of endocytosis from WT, DJ-1 KO and rescue neurons. ***$P = 2.0825 \cdot E^{-7}$. (*I*) Cumulative frequency of time constants from single synaptic bouton analysis of WT, DJ-1 KO and rescue neurons.

Reavailability Is Significantly Defective in DJ-1 KO Neurons. Since SV endocytosis is altered in DJ-1 KO neurons, we further explored presynaptic physiology under various conditions to determine whether endocytic defects influence other synaptic phenotypes. We examined exocytosis with application of 100-AP stimulus. Interleaved between test pulses, neurons were challenged with 300 AP (Fig. 4*A*, *Inset*). In WT neurons, the amplitudes of SV exocytosis following the first and second 300-AP challenge were slightly decreased (~15%) but similar in magnitude. In contrast, in DJ-1 KO neurons, amplitudes of SV exocytosis were significantly decreased after each challenge. This phenotype was reversed by expression of WT DJ-1 in DJ-1 KO neurons, implying that repetitive neural activity affects SV exocytosis (Fig. 4 *A* and *B*), leading to failure of recovery of these neurons from prolonged activity. Next, we investigated whether this finding is attributable to alteration of SV reavailability in DJ-1 KO neurons. To measure SV reavailability, we employed a FM1-43 loading and unloading strategy (21). Vesicle reavailability was assessed by tracing the time course of rerelease of internalized FM1-43 during a given stimulus. Our data clearly showed a decrease in the rerelease of FM1-43 in DJ-1 KO neurons, compared with that of WT neurons (Fig. 4 *C* and *D*), strongly suggesting that loss of DJ-1 leads to impairment of SV recycling, in particular, the kinetics of SV reavailability.

Expression of Familial Mutants of DJ-1 Fails to Rescue the Defective Endocytic Phenotype in DJ-1 KO Neurons. Several mutations of DJ-1 have been identified in early-onset familial PD (15). Considering that defects in SV recycling in DJ-1 KO neurons can be fully reversed by reexpression of WT DJ-1 protein (Fig. 3), we further determined whether these pathogenic mutations result in loss of function with respect to the ability to restore SV recycling kinetics. Neurons from DJ-1 KO mice were cotransfected with vG-pH as well as cDNA encoding DJ-1 harboring M26I, E64D,

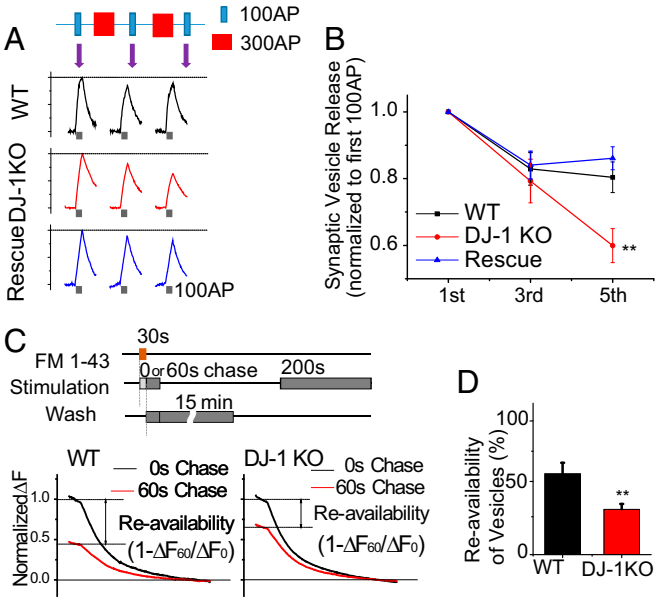

Fig. 4. DJ-1 is required for SV reavailability. (*A*) Representative traces of vG-pH responses to the first, third, and fifth stimulations (100 AP) during repetitive stimulation from WT (*Top*), DJ-1 KO (*Middle*), and rescue (*Bottom*) neurons. (*Inset*) Schematic diagram of repetitive stimulation. Blue indicates 100 AP and red indicates 300 AP at 10 Hz. (*B*) Mean values of normalized amplitude of response to the first, third, and fifth stimulations (100 AP) from WT (black), DJ-1 KO (blue), and rescue (red) neurons. [$WT_{100\ AP:first\text{-}third\text{-}fifth}$] = 1–0.83–0.80 (n= 15), [$DJ\text{-}1KO_{100\ AP:first\text{-}third\text{-}fifth}$] = 1–0.79–0.59 ($n$ = 15), [$Rescue_{100\ AP:first\text{-}third\text{-}fifth}$] = 1–0.84–0.86 ($n$ = 12). (*C*, *Upper*) Schematic diagram of FM1-43 loading and unloading protocol for the reavailability assay. (*C*, *Lower*) Representative traces of FM1-43 responses to a 60-s chase and 0-s chase in WT (*Left*) and DJ-1KO (*Right*) neurons. Reavailability was calculated as $1 - \Delta F_{60}/\Delta F_0$ (21). (*D*) Mean percentage reavailability from WT and DJ-1 KO neurons. Percentage was calculated as $(1 - \Delta F_{60}/\Delta F_0) \times 100$. WT = 53.30 ± 7.39% ($n$ = 8), DJ-1 KO = 29.84 ± 3.63% (n = 13), $^{**}P < 0.01$.

and L166P missense mutations, respectively. As shown in Fig. 5, defects in endocytosis observed in DJ-1 KO neurons were not rescued by expression of missense mutants of DJ-1. Endocytosis was slower by around twofold. Each set of neurons was reciprocally stained with anti-Flag antibody after live imaging. All Flag-tagged mutants were significantly expressed at the nerve terminals, although the signal of the L166P mutant was slightly weaker (Fig. 5 *G–I*). Thus, familial mutants of DJ-1 localize at the presynaptic boutons, comparable to WT DJ-1, but fail to function in SV endocytosis. Because DJ-1 is a known antioxidant or sensor of oxidative stress (22, 23), we further investigated whether the antioxidant effect of DJ-1 is involved in SV endocytosis. DJ-1 KO neurons transfected with the oxidative C106A mutant of DJ-1 and vG-pH were subjected to the SV endocytosis assay. Notably, SV endocytosis in C106A-expressing DJ-1 KO neurons was not impaired (Fig. S5). In addition, structural and functional aspects of mitochondria were also assessed in WT and DJ-1 KO neurons. An analysis of mitochondria structures, observed by monitoring Mito-Red fluorescence, showed that the relative distribution and shape of mitochondria at synaptic boutons, cell bodies, and dendrites were not significantly different between WT and DJ-1 KO neurons (Figs. S5 *D* and *E* and S6). Mitochondrial function was assessed by measuring synaptic ATP levels and mitochondrial membrane potential using exogenously introduced Syn-ATP (synaptic ATP sensor) (24) and tetramethylrhodamine ethyl ester (TMRE) (25), respectively. These analyses showed that synaptic ATP levels and mitochondrial membrane potential were also not significantly different between WT and DJ-1 KO neurons (Figs. S7 and S8). Our data suggest that DJ-1 mutations lead to a loss of function that affects the ability of the protein to sustain normal SV recycling kinetics, but the antioxidant role of DJ-1 may not be essential for SV endocytosis. Moreover, synaptic defects caused by DJ-1 ablation are not likely attributable to changes in mitochondrial distribution or morphology, or mitochondrial dysfunctions that affect ATP production or mitochondrial membrane potential.

Alterations in Cholesterol Level Caused by a DJ-1 Deficiency Affect SV Endocytosis. We previously reported that membrane lipid components were altered in the DJ-1 KO model, showing that DJ-1–deficient cells, including mouse embryonic fibroblasts (MEFs) and primary astrocytes, exhibited approximately a 20% decrease in cholesterol levels (26) in conjunction with an endocytic defect (26, 27). With this in mind, we reasoned that impairment of SV endocytosis in DJ-1 KO neurons was related to this alteration in cholesterol. To test this hypothesis, we first deprived WT and DJ-1 KO neurons of membrane cholesterol by treating them with methyl-β-cyclodextrin (MβCD) and subsequently monitoring SV endocytosis. These experiments showed that depletion of membrane cholesterol reduced the rate of SV endocytosis by ∼50% in WT neurons, but had only a modest effect in DJ-1 KO neurons (Fig. 6*A*). We then provided additional cholesterol by treating WT and DJ-1 KO neurons with soluble cholesterol, and measured SV endocytosis. Interestingly, this maneuver almost completely rescued the kinetics of SV endocytosis in DJ-1 KO neurons, restoring a near-WT phenotype. However, the addition of soluble cholesterol barely affected SV recycling in WT neurons, implying that a DJ-1 deficiency alters cholesterol levels in neurons, and this alteration, in turn, influences SV endocytosis.

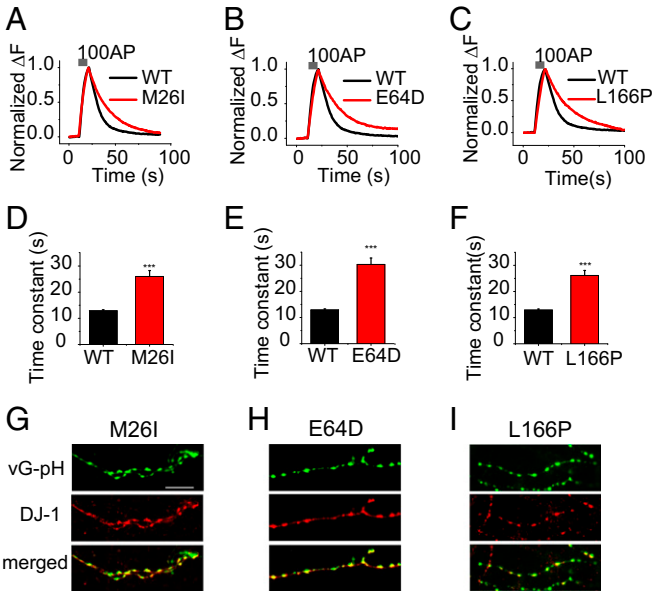

Fig. 5. Expression of familial mutants of DJ-1 fails to rescue defects in SV endocytosis in DJ-1 KO neurons. (*A–C*) Representative trace of vG-pH responses to 100 AP from DJ-1 M26I (*A*), DJ-1 E64D (*B*), and DJ-1 L166P (*C*) -expressing neurons. (*D–F*) Mean poststimulus endocytic time constants from (*D*) DJ-1 M26I (τ_{endo} = 26.01 ± 2.25 s; n = 10), (*E*) DJ-1 E64D (τ_{endo} = 30.3 ± 2.44 s; n = 14), and (*F*) DJ-1 L166P (τ_{endo} = 26.11 ± 1.92 s; n = 13) -expressing neurons. $^{***}P < 0.001$ (*G–I*) Representative images of DJ-1 mutant expression in DJ-1 KO neurons. Neurons transfected with Flag-tagged DJ-1 mutants (*G*, M26I; *H*, E64D; *I*, L166P) were retrospectively fixed and stained with anti-Flag antibody after the vG-pH assay. (Scale bar, 5 μm.)

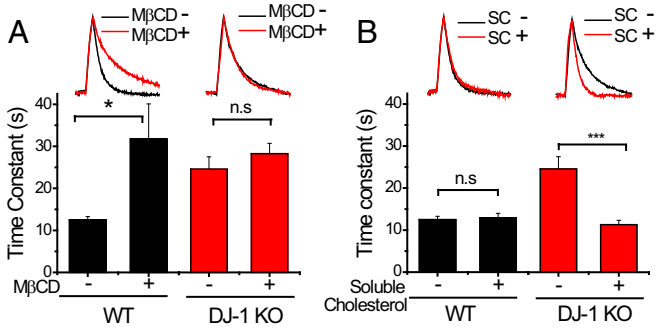

Fig. 6. Alterations in cholesterol levels in DJ-1 KO neurons influence SV recycling. (*A*, *Upper*) Representative trace of vG-pH responses to 100 AP in the presence and absence of MβCD in WT (*Lower*, *Left*) and DJ-1 KO (*Lower*, *Right*) neurons. Neurons were treated with MβCD (1 mM) for 4 h, and SV endocytosis was monitored. Data represent mean values of endocytic time constants for WT and DJ-1 KO neurons in the absence or presence of MβCD. WT: $M\beta CD^-$ τ_{endo} = 12.5 ± 0.79 s (n = 11), $M\beta CD^+$ τ_{endo} = 31.72 ± 8.37 s (n = 10); DJ-1 KO: $M\beta CD^-$ τ_{endo} = 24.59 ± 2.92 s (n = 18), $M\beta CD^+$ τ_{endo} = 28.27 ± 2.44 s (n = 20). (*B*, *Upper*) Representative trace of vG-pH responses to 100 AP in the presence and absence of soluble cholesterol (SC) in WT (*Lower*, *Left*) and DJ-1 KO (*Lower*, *Right*) neurons. Neurons were incubated with soluble cholesterol (200 μg/mL) overnight (8–12 h), and SV endocytosis was subsequently monitored. Data represent mean values of endocytic time constants in WT and DJ-1 KO neurons in the absence or presence of soluble cholesterol (SC). WT: SC^- τ_{endo} = 12.5 ± 0.79 s (n = 11), SC^+ τ_{endo} = 12.89 ± 1.11 s (n = 6); DJ-1 KO: SC^- τ_{endo} = 24.59 ± 2.92 s (n = 18), SC^+ τ_{endo} = 11.33 ± 1.02 s (n = 8). ***P < 0.001, *P < 0.05; n.s, not significant.

Discussion

Accumulating evidence indicates that the gene products causing familial PD operate through common molecular pathways that trigger neuronal degeneration (28–30). Our data strongly support the notion that DJ-1 participates in SV endocytosis, and alterations in this process induced by familial mutants of DJ-1, may be a conversant pathology in the pathogenesis of PD.

DJ-1 is localized at presynaptic terminals, which is in agreement with previous studies (16, 17). Although ultrastructural studies have shown that DJ-1 is not involved in structural processes of nerve terminals, a highly sensitive functional presynaptic assay with vG-pH revealed that DJ-1 participates in SV endocytosis and reavailability. A DJ-1 deficiency leads to a decrease in the rate of SV endocytosis without affecting exocytosis. Repetitive neural activity in DJ-1 KO neurons ultimately impairs synaptic transmission. Reexpression of WT DJ-1 rescued the defect in SV endocytosis and reavailability characteristic of DJ-1 KO neurons. Additionally, our study showed that mutants of DJ-1 identified in familial PD reach the synaptic boutons, as does WT DJ-1. Although the DJ-1 L166P mutant showed less localization to synaptic boutons compared with WT DJ-1 and other mutants, this might be attributable to decreased stability of this mutant (31, 32). Nevertheless, familial mutants of DJ-1 failed to rescue the defect in SV endocytosis in DJ-1 KO neurons. Mutations of DJ-1 identified in familial PD induce structural alterations to varying degrees (33) and are predicted to cause a loss of function, a finding that is also applicable to the synaptic role of DJ-1. One potential mechanism by which DJ-1 may act is through modulation of the balance of membrane cholesterol levels at synapses.

Several intriguing questions arise from this study. First, is the defect in SV endocytosis and reavailability in DJ-1 KO neurons specific to the synapse? Are other membrane trafficking systems, such as endosomes and lysosomes, also affected? Our brief survey of structural aspects of early endosomes (using Rab5) and lysosomes (using Lamp-1) showed that the distribution of these proteins was not particularly different (Fig. S9). Although there is one report that a DJ-1 deficiency reduces lysosomal activity (34), additional studies will be required to confirm this. Second, how well do our results correlate with in vivo findings? Although it has been reported that a DJ-1 deficiency causes age-dependent motor deficits (35) and hypokinesia (36), it is generally thought that there is no associated behavioral defect or a very modest one. There are several possible explanations for the discrepancy between the general absence of a behavioral phenotype and an SV endocytic defect. One possibility relates to the frequency of neuronal activity. Neurons lacking DJ-1 exhibited slowed endocytosis and defects in reavailability that were associated with a decrease in release after repetitive neural activity over a short time window (1–3 min). In this case, the efficiency of SV reuse was insufficient to keep pace in the context of rapid, high neural activity. If sparse neural activity occurs with an intermission long enough to allow recycling and reuse of SVs in DJ-1 KO neurons, synaptic-rundown effects could be discounted. In fact, we tested this model in WT and DJ-1 neurons, and found that the rundown of synaptic transmission disappeared with a long intermission (10 min) between neural activity (100 AP) (Fig. S10). In future studies, it would be interesting to perform behavioral tests in DJ-1 KO mice under various conditions, including long-lasting neural activity (e.g., continual motor activity). Third, what are the molecular mechanisms underlying the defective SV endocytosis observed in DJ-1 KO neurons? Our first tests using the antioxidant-defective DJ-1 mutant, C106A, revealed that oxidative stress is not involved in the SV endocytic defect in DJ-1 KO neurons. Additionally, mitochondrial structure and function (ATP, membrane potential) were normal in DK-1 KO neurons. A previous study reported that membrane lipid components are altered in DJ-1 KO cells (e.g., MEFs and astrocytes), with consequent effects on membrane fluidity (26). We tested SV endocytosis by modulating the level of cholesterol, one of the key lipids in the membrane. Depleting cholesterol impaired SV endocytosis in WT neurons, but not in DJ-1 KO neurons. Conversely, adding cholesterol restored SV endocytosis in DJ-1 KO neurons, but produced no additive effect on SV endocytosis in WT neurons. Because cholesterol is a major lipid component of cellular membranes and regulates the degree of membrane fluidity (37), these findings suggest that DJ-1–mediated balancing of cholesterol levels may influence SV endocytosis by regulating synaptic membrane fluidity. Notably, synapses are enriched in cholesterol (38), which has been implicated in the regulation of synaptic endocytosis (39); however, the mechanistic details of the process by which cholesterol regulates SV endocytosis remain elusive. Possible directions for future research include modulating lipid content of SV membranes and plasma membranes in DJ-1 KO neurons, performing correlations with other genetic factors of PD, and exploring other potential mechanisms of DJ-1 in SV recycling.

In addition to DJ-1, several other familial factors associated with PD are directly or indirectly linked to SV endocytosis. For example, the balance in the amount of synuclein in nerve terminals is critical for endocytosis (40, 41). Moreover, endogenous LRRK2 modulates SV endocytosis (8, 9) and has been shown to genetically and biochemically interact with endophilin, a protein critically involved in SV endocytosis (42). Parkin expression is also tightly associated with that of endophilin (6). Recently, a mutant *Synj1* knock-in mouse, identified in patients with early-onset atypical parkinsonism (10, 11), displays phenotypes that recapitulate parkinsonism with seizures (43). Taken together, these findings indicate that endocytic dysfunction is associated with the pathogenesis of PD and parkinsonism. The next challenge will be to determine how impairments in SV endocytosis are physically connected to processes that cause PD or parkinsonism, and how they are related to specific types of neurons, such as DAergic neurons in the substantia nigra pars compacta, which is highly susceptible to loss in PD.

Materials and Methods

DJ-1 KO mice were kindly provided by U. J. Kang at the Department of Neurology, University of Chicago, Chicago, IL (35), and all experimental

procedures (including animal protocols) were conducted according to the guidelines established by the Ajou University School of Medicine Ethics Review Committee for Animal Experiments (2014-0048). All experimental procedures, such as primary cortical culture, optical imaging, image analysis, and electron microscopy are described in *SI Materials and Methods*.

ACKNOWLEDGMENTS. We thank Dr. Timothy A. Ryan (Department of Biochemistry, Weill Cornell Medical College) for critical reviewing of the manuscript and providing Syn-ATP plasmid; members of the S.H.K. and the S.M.P. laboratories for their valuable comments; and Young-Jae Ryu and Chang-man Ha for helping superresolution imaging supported by Brain Research Core Facilities in the Korea Brain Research Institute. This work was supported by the Medical Research Center Program National Research Foundation of Korea Grant NRF-2012R1A5A2048183 (to S.M.P.); Basic Science Research Programs 2015R1A2A2A01007457 (to S.M.P.) and 2017R1A2B4007019 (to S.H.K.); Brain Research Program 2016M3C7A1905074 (to S.H.K.) through the National Research Foundation of Korea (NRF); and Korea Brain Research Institute basic research program 17-BR-01 (to S.H.K.) funded by the Ministry of Science and Information and Communication Technology.

1. Kalia LV, Lang AE (2015) Parkinson's disease. *Lancet* 386:896–912.
2. Picconi B, Piccoli G, Calabresi P (2012) Synaptic dysfunction in Parkinson's disease. *Adv Exp Med Biol* 970:553–572.
3. Nemani VM, et al. (2010) Increased expression of alpha-synuclein reduces neurotransmitter release by inhibiting synaptic vesicle reclustering after endocytosis. *Neuron* 65:66–79.
4. Wang L, et al. (2014) α-synuclein multimers cluster synaptic vesicles and attenuate recycling. *Curr Biol* 24:2319–2326.
5. Vargas KJ, et al. (2014) Synucleins regulate the kinetics of synaptic vesicle endocytosis. *J Neurosci* 34:9364–9376.
6. Cao M, Milosevic I, Giovedi S, De Camilli P (2014) Upregulation of Parkin in endophilin mutant mice. *J Neurosci* 34:16544–16549.
7. Trempe JF, et al. (2009) SH3 domains from a subset of BAR proteins define a Ubl-binding domain and implicate parkin in synaptic ubiquitination. *Mol Cell* 36: 1034–1047.
8. Arranz AM, et al. (2015) LRRK2 functions in synaptic vesicle endocytosis through a kinase-dependent mechanism. *J Cell Sci* 128:541–552.
9. Maas JW, Yang J, Edwards RH (2017) Endogenous leucine-rich repeat kinase 2 slows synaptic vesicle recycling in striatal neurons. *Front Synaptic Neurosci* 9:5.
10. Quadri M, et al.; International Parkinsonism Genetics Network (2013) Mutation in the SYNJ1 gene associated with autosomal recessive, early-onset Parkinsonism. *Hum Mutat* 34:1208–1215.
11. Krebs CE, et al. (2013) The Sac1 domain of SYNJ1 identified mutated in a family with early-onset progressive Parkinsonism with generalized seizures. *Hum Mutat* 34: 1200–1207.
12. Köroğlu Ç, Baysal L, Cetinkaya M, Karasoy H, Tolun A (2013) DNAJC6 is responsible for juvenile parkinsonism with phenotypic variability. *Parkinsonism Relat Disord* 19: 320–324.
13. Edvardson S, et al. (2012) A deleterious mutation in DNAJC6 encoding the neuronal-specific clathrin-uncoating co-chaperone auxilin, is associated with juvenile parkinsonism. *PLoS One* 7:e36458.
14. Trinh J, Farrer M (2013) Advances in the genetics of Parkinson disease. *Nat Rev Neurol* 9:445–454.
15. da Costa CA (2007) DJ-1: A newcomer in Parkinson's disease pathology. *Curr Mol Med* 7:650–657.
16. Olzmann JA, et al. (2007) Selective enrichment of DJ-1 protein in primate striatal neuronal processes: Implications for Parkinson's disease. *J Comp Neurol* 500:585–599.
17. Usami Y, et al. (2011) DJ-1 associates with synaptic membranes. *Neurobiol Dis* 43: 651–662.
18. Voglmaier SM, et al. (2006) Distinct endocytic pathways control the rate and extent of synaptic vesicle protein recycling. *Neuron* 51:71–84.
19. Kim SH, Ryan TA (2009) Synaptic vesicle recycling at CNS snapses without AP-2. *J Neurosci* 29:3865–3874.
20. Kim SH, Ryan TA (2010) CDK5 serves as a major control point in neurotransmitter release. *Neuron* 67:797–809.
21. Mani M, et al. (2007) The dual phosphatase activity of synaptojanin1 is required for both efficient synaptic vesicle endocytosis and reavailability at nerve terminals. *Neuron* 56:1004–1018.
22. Canet-Avilés RM, et al. (2004) The Parkinson's disease protein DJ-1 is neuroprotective due to cysteine-sulfinic acid-driven mitochondrial localization. *Proc Natl Acad Sci USA* 101:9103–9108.
23. Meulener MC, Xu K, Thomson L, Ischiropoulos H, Bonini NM (2006) Mutational analysis of DJ-1 in *Drosophila* implicates functional inactivation by oxidative damage and aging. *Proc Natl Acad Sci USA* 103:12517–12522, and erratum (2006) 103:14978.
24. Rangaraju V, Calloway N, Ryan TA (2014) Activity-driven local ATP synthesis is required for synaptic function. *Cell* 156:825–835.
25. Cai Q, Zakaria HM, Simone A, Sheng ZH (2012) Spatial parkin translocation and degradation of damaged mitochondria via mitophagy in live cortical neurons. *Curr Biol* 22:545–552.
26. Kim J-M, et al. (2016) DJ-1 deficiency impairs glutamate uptake into astrocytes via the regulation of flotillin-1 and caveolin-1 expression. *Sci Rep* 6:28823.
27. Kim KS, et al. (2013) DJ-1 associates with lipid rafts by palmitoylation and regulates lipid rafts-dependent endocytosis in astrocytes. *Hum Mol Genet* 22:4805–4817.
28. Park J, et al. (2006) Mitochondrial dysfunction in *Drosophila* PINK1 mutants is complemented by parkin. *Nature* 441:1157–1161.
29. Greggio E, Bisaglia M, Civiero L, Bubacco L (2011) Leucine-rich repeat kinase 2 and alpha-synuclein: Intersecting pathways in the pathogenesis of Parkinson's disease? *Mol Neurodegener* 6:6.
30. Kamp F, et al. (2010) Inhibition of mitochondrial fusion by α-synuclein is rescued by PINK1, Parkin and DJ-1. *EMBO J* 29:3571–3589.
31. Moore DJ, Zhang L, Dawson TM, Dawson VL (2003) A missense mutation (L166P) in DJ-1, linked to familial Parkinson's disease, confers reduced protein stability and impairs homo-oligomerization. *J Neurochem* 87:1558–1567.
32. Olzmann JA, et al. (2004) Familial Parkinson's disease-associated L166P mutation disrupts DJ-1 protein folding and function. *J Biol Chem* 279:8506–8515.
33. Malgieri G, Eliezer D (2008) Structural effects of Parkinson's disease linked DJ-1 mutations. *Protein Sci* 17:855–868.
34. Krebiehl G, et al. (2010) Reduced basal autophagy and impaired mitochondrial dynamics due to loss of Parkinson's disease-associated protein DJ-1. *PLoS One* 5:e9367.
35. Chen L, et al. (2005) Age-dependent motor deficits and dopaminergic dysfunction in DJ-1 null mice. *J Biol Chem* 280:21418–21426.
36. Goldberg MS, et al. (2005) Nigrostriatal dopaminergic deficits and hypokinesia caused by inactivation of the familial Parkinsonism-linked gene DJ-1. *Neuron* 45:489–496.
37. Spector AA, Yorek MA (1985) Membrane lipid composition and cellular function. *J Lipid Res* 26:1015–1035.
38. Puchkov D, Haucke V (2013) Greasing the synaptic vesicle cycle by membrane lipids. *Trends Cell Biol* 23:493–503.
39. Wasser CR, Ertunc M, Liu X, Kavalali ET (2007) Cholesterol-dependent balance between evoked and spontaneous synaptic vesicle recycling. *J Physiol* 579:413–429.
40. Xu J, et al. (2016) α-Synuclein mutation inhibits endocytosis at mammalian central nerve terminals. *J Neurosci* 36:4408–4414.
41. Vargas KJ, et al. (2017) Synucleins have multiple effects on presynaptic architecture. *Cell Rep* 18:161–173.
42. Matta S, et al. (2012) LRRK2 controls an EndoA phosphorylation cycle in synaptic endocytosis. *Neuron* 75:1008–1021.
43. Cao M, et al. (2017) Parkinson Sac domain mutation in synaptojanin 1 impairs clathrin uncoating at synapses and triggers dystrophic changes in dopaminergic axons. *Neuron* 93:882–896.e885.